

Research and Innovation action

NUMBER — 955387 — LEON-T

LEON-T

Low particle Emissions and lOw Noise Tyres



Deliverable No.	3.3	
Deliverable Title	UV-degradation and analysis of tyre and road wear particles (TRWP)	
Dissemination	PU	
Written by	Luke Parker, Marloes van Os, Elena Höppener, Peter Tromp, Arjen Boersma and Alex van Renesse van Duivenbode (all TNO)	11/12/2023
Checked by	Joris T.K. Quik (RIVM)	00/00/0000
Approved by	Name (Affiliation)	00/00/0000
Issue date	00/00/0000	



This Project has received funding from the European Union's Horizon 2020 research and innovation programme under grant agreement N° 955397. The content of this report reflects only the author's view CINEA is not responsible for any use that may be made of the information it contains.

Revision History

REVISION	DATE	DESCRIPTION	AUTHOR (ORGANIZATION)
0	11/12/2023	First draft prepared by TNO	Luke Parker (TNO)
1	08/01/2024	Revisions by WP leader	Joris Quik (RIVM)
2	06/03/2024	Revisions by consortium leader	Juan Jesus García (IDIADA)
3	16/04/2024	Internal TNO approval process	Sieger Henke/Jorien Strijk (TNO)

Contents

1	INTRODUCTION	5
2	RESULTS AND DISCUSSION	6
2.1	Degradation Rate of T(R)WPs	6
2.2	Effect of Ageing on T(R)WP Size	8
2.3	Morphology and Elemental Composition of (Aged) T(R)WPs	10
3	CONCLUSIONS	12
4	BIBLIOGRAPHY	14
5	APPENDIX.....	16
5.1	Experimental methods and materials	16
5.2	Supplementary information TGA	17
5.3	Supplementary information SEM	18

Abbreviations and Units

BR	Butadiene Rubber
BSE	Back Scattered Electrons
CB	Carbon Black
DTG	Differential Thermogravimetry
EC	Elemental Carbon
EDX	Energy-dispersive X-ray spectroscopy
LN ₂	Liquid Nitrogen
NR	Natural Rubber
PM	Particulate Matter
SBR	Styrene Butadiene Rubber
SE	Secondary Electrons
SEM	Scanning Electron Microscope
SEM-EDX	Scanning Electron Microscopy with Energy-Dispersive X-ray spectroscopy
SLS	Static Light Scattering
SVOC	Semi-Volatile Organic Compounds
TGA	Thermogravimetric analysis
T(R)WP	Tyre (and Road) Wear Particles
TWP	Tyre Wear Particles

1 Introduction

Tyre and road wear particles (TRWPs) are an environmental contaminant of high concern due to their high abundance and wide environmental distribution (1–6). They are predicted to be the largest source of microplastics with annual global emissions estimated to be between 800–3300 kt (5, 6). TRWPs are a form of non-exhaust vehicle emissions (NEE) that have been recognised as a growing problem and are expected to be regulated in upcoming Euro 7 legislation. TRWPs are generally described as elongated particles with a heterogeneous composition of tyre tread with encrustations of traffic related particles such as brake and road wear (4, 7–10). Tyre tread consists for ~50% of synthetic and natural rubbers while the rest of the weight is due to softeners, vulcanisation agents, fillers and various other additives (4).

Several factors affect the environmental fate of TRWPs. Transport is affected by their size: small particles will be dispersed in the air, whilst large particles will deposit on or near the road surface after which they are further transported through resuspension and run-off to road side soils, sewers and surface waters (6, 11). According to Baensch-Baltruschat *et al.*, 66–76% of the coarse ‘non-airborne’ fraction is transported to soils and road banks near roads and 12–20% is released to surface waters (11). This is comparable with estimates in the Netherlands showing that 6% is directly ending up in surface waters, 15% in sewers and 67% in soil (12), and a Swiss study estimated that 74% is deposit in roadside soils and 22% in surface waters (13). As the most TRWPs are estimated to end up in roadside soils, understanding environmental fate of TRWPs in this compartment is of great importance. However limited information is available on the degradation of TRWP in soils (6, 11).

Often modelling studies are used to better understand the environmental fate and transport of TRWPs (14, 15). An important variable in these models is how fast TRWPs degrade in the different environmental compartments. Both photo- and biodegradation are relevant degradation paths to consider. Cadle and Williams studied the environmental degradation of T(R)WPs in soil including factors such as oxygen, heat, humidity, light and microorganisms in real-time, using an open set-up exposed to the elements (14). They found that degradation of tyre wear in soil had a rate of 0.15% per day and noted that the presence of microbes and type of tyre material (tread vs wear) play a big role in degradation. For unvulcanised rubber they conclude that oxidation processes are more significant than microbial degradation processes (14, 16). While some work has given mechanical insights that rubbers such as polystyrene-butadiene and poly-isoprene undergo photodegradation (17), the studies of Cadle and Williams remains the only one to provide a degradation rate. Recent lab-scale investigations into the effects of photodegradation also do not report degradation rates as these have focussed on the effects on leaching and transformation of tyre additives (18, 19).

The degradation rates used in the currently available modelling studies are mostly based on the research of Cadle and Williams from 1980 (14, 15). As Corella-Puertas *et al.* mention, this is the only experimental study to provide a half-life of tire wear particles in soil and there are no studies on the degradation of TRWP in the aquatic environment (20). As the composition of tyres has changed over the 40 years since the study, the results of Cadle and Williams may be less relevant now than when they were first published. Therefore, updated degradation rates for TRWP would result in a big improvement in the accuracy of modelling. Combining this with state of the art physicochemical characterisation of TRWPs as a result of ageing will further contribute towards understanding particle transport.

The aim of this research is to characterise the effect of UV-degradation on TRWP and provide updated degradation rates for TRWPs. To achieve this, samples have been aged following an accelerated UV-ageing procedure. To test the degradation of pure tyre tread, tyres have been cryomilled, which is recognized as an efficient method to reduce the particle size of rubber (18, 21). It has also been reported that the wear process that generates TRWPs under real conditions also causes significant chemical changes in the tread rubber, with studies showing that more rubber is unvulcanised so the material absorbs oxygen much faster than tread rubber which has been cryomilled to the same particle size (14). To investigate the effects of realistic wear, we use simulated TRWP generated at a road simulator. Thermogravimetric analysis (TGA) is used to investigate the degradation rate whilst static light scattering (SLS), electron microscopy (SEM-EDX) and infrared (FTIR) are used to characterise the physicochemical changes of the particles due to UV-ageing.

2 Results and Discussion

In this research, four T(R)WP samples were used and these are summarised in Table 1. Two samples of tyre wear particles (TWPs) were prepared by cryogenic milling to investigate the effects of UV degradation purely on tyre material. A mix of light duty (car/van) tyres and heavy duty (truck) tyres were compared as the former contains more synthetic rubber and the latter more natural rubber. The other two samples were prepared by running tyres on a road simulator and collecting the TRWPs generated. This allows for investigation of more realistic particles that also include road wear encrustations. TRWPs were prepared from the same mix of light duty tyres, which were from the executive market segment, as the cryomilled car TWPs in order to investigate the influence of road wear encrustations and the wear process. TRWPs were also collected from a budget segment light-duty tyre, which contains different fillers and rubber formulations. Finally, all samples were sieved to a size fraction of 50 – 200 µm to be representative of T(R)WPs that are deposited in roadside soils, the environmental compartment with the most T(R)WPs.

Table 1. Summary of T(R)WPs samples used in this study.

Sample Name	Preparation Method	Tyre Details
Car TWPs	Cryomilling	Mix of four new executive segment tyres
Truck TWPs	Cryomilling	Mix of shredded end-of-life truck tyres from tyre recycler
Premium TRWPs	Road Simulator	Mix of four new executive segment tyres
Budget TRWPs	Road Simulator	One new budget segment tyre

T(R)WPs were subjected to accelerated photothermal ageing (for details see methods section; Appendix 5.1) with samples taken for characterisation at four time points (0, 160, 505 and 1000 h). For converting the accelerated exposure in the UV cabinet to environmentally relevant figures, the intensity of the UV light and the temperature need to be compared with natural conditions. Since we have only done UV ageing experiments at one temperature and one UV intensity, two assumptions were made: that thermal activation increases by a factor of 2 for every 10 °C and that UV-activation increases linearly. This leads to a total acceleration factor of 24. Given 1000 h of accelerated ageing and assuming an average sunshine exposure of 8 h per day in the environment, this leads to a simulated environmental ageing time of 8.2 years. This value has been used for calculating environmental degradation rates. As this has a large degree of error, degradation rates have been provided in brackets to show a range from 5-10 environmental years.

2.1 Degradation Rate of T(R)WPs

Thermogravimetric Analysis (TGA) was used to investigate the degradation rate of T(R)WPs. As different components of T(R)WP will be lost at specific temperatures it is possible to determine the composition of the different samples and how this changes with ageing.

The composition of the four samples as determined by TGA is shown in Table 2. The composition is expected for standard tyres, namely 40-60% rubber, 20-30% filler (SiO₂ or carbon black (CB)) and 12-15% oils (8). The car TWPs prepared by cryomilling have a much higher inert fraction compared to Truck TWPs. This is due to the inclusion of SiO₂ as a mineral filler in car tyres and for truck tyres CB is the main filler. The two TRWP samples have much higher inert fractions due to the presence of road wear particles which are mainly aluminium and silicon-rich minerals.

Table 2. Composition of T(R)WP samples as determined by TGA.

	Volatiles	Rubber	Carbon Black	Inert
Car TWPs	6.5	52.8	4.1	36.6

D3.3 UV-degradation and analysis of tyre and road wear particles (TRWP) - PU

Truck TWPs	4.6	60.8	29.0	5.6
Premium TRWPs	1.6	10.1	6.5	81.9
Budget TRWPs	1.5	7.6	5.7	85.2

Figure 1A shows the TGA trace of the car tyre sample in black with the different components annotated on the right-hand side (plots for the other samples are available in the Supplementary Information, Figure S1). There is a gradual weight loss until $\sim 290^\circ\text{C}$, which is due to the evaporation of semi-volatile organics present such as softeners, vulcanisation agents and antioxidants. From $290 - 550^\circ\text{C}$ there is a sharp weight loss event due to pyrolysis of tyre rubber. At 750°C , the nitrogen environment is changed to air and this leads to a weight loss event at $\sim 800^\circ\text{C}$ due to the oxidation of carbon black. The remaining weight is referred to as inert material or ash and this is mainly due to SiO_2 filler.

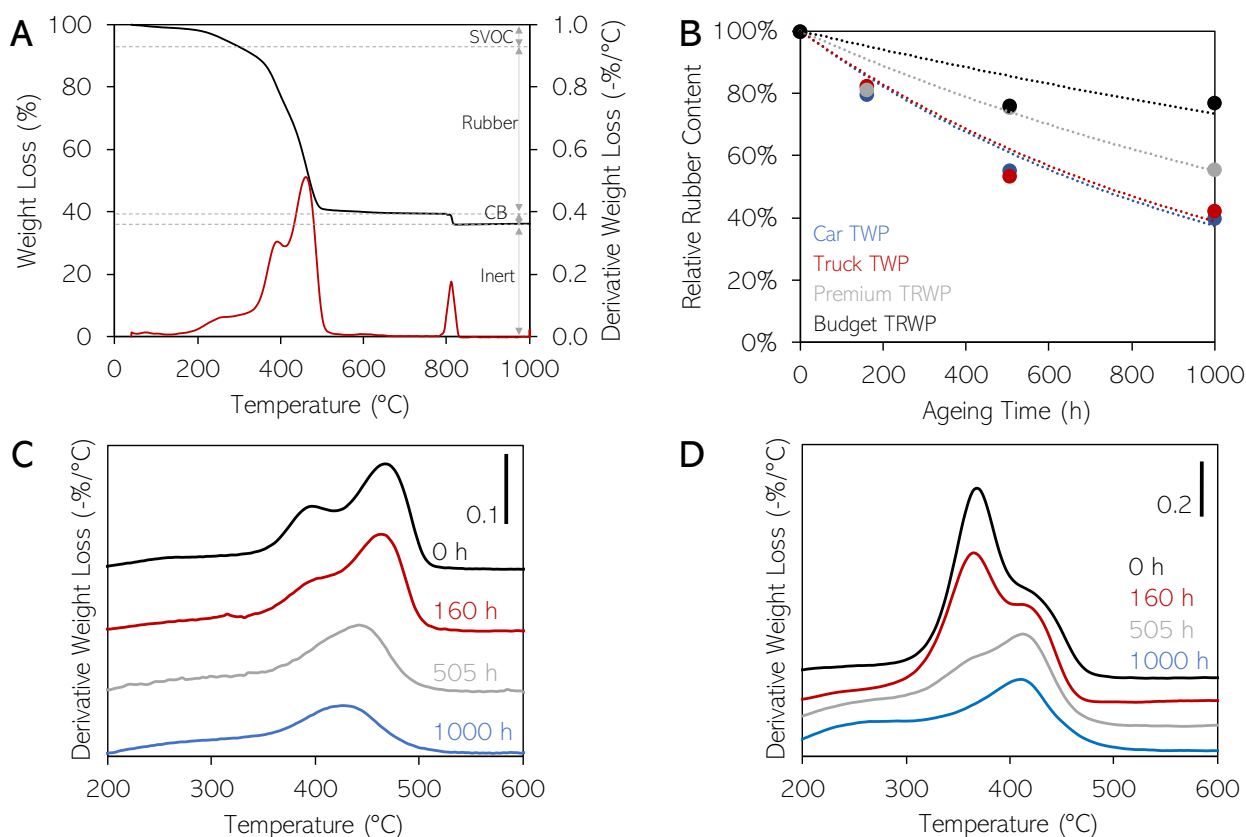


Figure 1. A. TGA (black) and DTG (red) plots of the Car TWPs sample before ageing; B. Rubber concentration of the four T(R)WP samples as a function of ageing time; C. DTG peaks of rubber for the Car TWPs sample at the four ageing times; and D. DTG peaks of rubber for the Truck TWPs sample at the four ageing times.

The red line in Figure 1A shows the differential of the TGA trace (DTG) curve (black line). Using the differential, small changes in composition are elucidated. For example, the weight loss between $290 - 550^\circ\text{C}$ due to rubber is shown to actually contain two events centred $\sim 390^\circ\text{C}$ and $\sim 480^\circ\text{C}$. Previous work has shown that different types of rubber pyrolyse at different temperatures and these two peaks correspond to natural rubber (NR) and synthetic rubber (SBR+BR), respectively (22).

The rubber degradation of the four different samples is shown Figure 1B. The cryomilled car tyres and truck tyres appear to very similar degradation rates of 0.033 (0.027 - 0.054) and 0.032 (0.026 - 0.052) day^{-1} , respectively. The samples from the road simulator had a much slower degradation rate. This is contrary to previous work that suggests

that particles formed through wear absorb oxygen faster. The premium TRWPs which are the same tyres as the car TWP sample but run on the road simulator, had a degradation rate of 0.020 (0.016 – 0.032) day⁻¹. Finally, the budget TRWPs show the slowest degradation of 0.011 (0.009 – 0.017) day⁻¹. Cadle and Williams studied unaccelerated environmental degradation by exposing TWPs and TRWPs in soil and glass beads for a period of 16 months. The TWPs and TRWPs in glass beads are assumed to be representative of unaccelerated abiotic degradation and may be compared with the Car TWP and two TRWPs in this study. The TWP in the previous study showed no degradation, whilst in this study they show the fastest. TRWPs in glass showed a degradation rate of 0.09 day⁻¹ which is approximately 5-10x faster than the TRWP samples in this study. Cadle and Williams also showed that degradation in soil was roughly twice as fast (0.15 day⁻¹) highlighting the important role biodegradation plays in the environmental fate of T(R)WPs.

The degradation rate is likely influenced by the type of rubber present in the tyres. As mentioned previously, using the DTG plot we can identify both natural and synthetic rubber. In Figure 1C, the rubber region of the DTG plot for cryomilled car tyres is shown with increasing ageing time. The fresh sample shows two peaks, *ca.* 390 °C and *ca.* 480 °C which have been shown to be due to NR and SBR+BR, respectively. It appears that the two types of rubber degrade at different rates, with the peak due to NR becoming indistinguishable after 500 h ageing. There also appears to be a shift of the synthetic rubber peak to lower temperatures with increased ageing, with the peak being centred around 430 °C after 1000 h ageing. This may be due to a chemical change in rubber occurring during ageing, such as devulcanization, that lowers the degradation temperature of the rubber. The aged truck tyres also show two peaks, as shown in Figure D, this time *ca.* 390 °C and *ca.* 435 °C. The shifted degradation temperature of the synthetic rubber with respect to that in the car tyres may be due to a different type or ratio of synthetic rubber(s) or, as these are end-of-life tyres, a different degree of vulcanisation. It is evident from the DTG that truck tyres contain a much larger proportion of natural rubber than synthetic rubber and this is again seen to degrade much quicker than the synthetic rubber.

2.2 Effect of Ageing on T(R)WP Size

It is also important to understand what influence degradation has on the physicochemical properties of T(R)WPs. This is of importance as a change in particle size will lead to different environmental transport behaviour, such as sedimentation rate in water and (re)suspension in air affecting long-range transport. It is also expected that smaller particles will be easier taken up by biota and present a potentially higher health effect. Static light scattering (SLS) was used to investigate changes in particle size with ageing and these are shown in Figure 2.

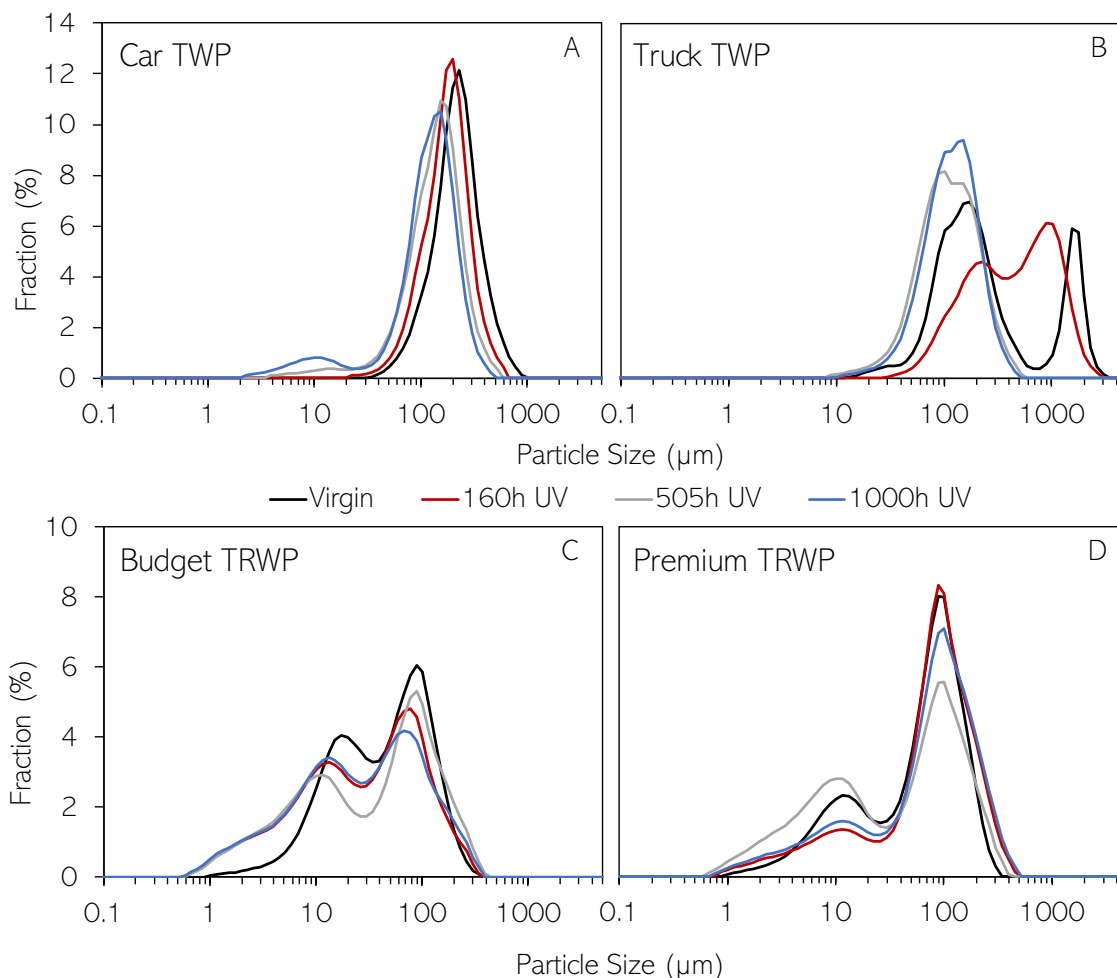


Figure 2. Volume distribution measured with Static Light Scattering (SLS) from **A.** Car TWP, **B.** Truck TWP, **C.** Budget TRWP and **D.** Premium TRWP. Each graph shows four lines that correspond to different ageing times: virgin (black), 160 h (red), 505 h (grey) and 1000 h (blue).

The modal particle size of the virgin car tire sample (Figure 2A) lies around 200 µm which is representative of the coarser TRWPs found in roadside soils. When looking at the samples that have been aged, the modal size of the TWPs clearly shifts to lower particle size with longer UV-exposure. From this we can calculate a particle size reduction rate of -0.03 ($0.02 - 0.05$) $\mu\text{m day}^{-1}$. A peak is also seen emerging around 10 µm and this peak intensifies as the sample has been aged longer. This bimodal distribution suggests that both surface degradation and fragmentation play a role.

The modal particle size of the truck tire sample (B) is similar to the one of the car tire sample, around 175 µm. However, the virgin sample also seems to have a part of the fraction with particle size larger than 1 mm. This could indicate the formation of agglomerates in the sample, even though a surfactant was added before analysis to prevent this. The “stickiness” of natural rubber containing truck tyres has previously been reported as a limiting factor in the particle size analysis of truck tyre cryogrinds (18). The sample that has been aged for 160 hours also shows a bimodal distribution, however, the 505 and 1000 h samples have a monomodal distribution. This is in line with the differential thermogravimetry (DTG) data presented earlier which showed that NR was almost completely degraded after 505 h ageing and the sample is predominantly synthetic rubber. It could also be that the surface of the particles changes such that agglomerates are less likely to form after ageing by UV-light, for example through formation of carbonyl groups increasing hydrophilicity. Furthermore, after ageing more than 500 hours, the tail of the peak starts to shift to lower particle sizes, which indicates the formation of more particles around 10 µm.

A difference between the milled TWP distributions and the budget (C) and premium (D) TRWP distributions, is the bimodal distribution of the unaged TRWP. Since the smaller particles are not present in the TWP samples, this could represent loose road wear in the sample. Whilst the samples were fractionated to between 53 – 200 μm during preparation, ultrasonic treatment during dispersion for SLS measurement could liberate loosely bound road wear encrustations from the TRWPs. The budget TRWP sample (C) shows a shift of the distribution towards smaller particle sizes. The fraction of particles *ca.* 100 μm is decreasing with longer degradation times, whilst the fraction of particles smaller than 10 μm is increasing. Different from the milled tire samples, nanoparticles <1 μm are also formed with longer UV exposure time. This increase in particles <1 μm is also clearly visible in the premium TRWP sample (D), however, these distributions do not show a clear shift like the other samples.

2.3 Morphology and Elemental Composition of (Aged) T(R)WPs

In the SLS results we see in many samples the size fraction <10 μm growing. For the car tire sample we can say with certainty that these particles originate from tire material, however for the TRWP samples it is not possible to say whether this fraction is due to rubber, road wear, or both. With SEM-EDX we can investigate both the morphology and elemental composition of individual particles, which may shed more light on this important smaller fraction.

In Figure 3A particles from <10 μm in the 1000 h aged car TWP sample are shown, together with their EDX spectrum in Figure 3B. The SEM analysis confirms the SLS results that there are a considerable number of particles <10 μm present in the sample. EDX analysis shows that these particles consist of a mixture of carbon (C), oxygen (O) and silicon (Si). The two Au peaks present are due to the gold-coated filters used to prepare the samples.

The SLS results show that the TRWP samples from the road simulator also contain particles <10 μm which is again confirmed by SEM analysis. However, not all of these particles have the same elemental composition. Figure 3C presents an elemental mapping of the particles in the premium TRWP sample after 1000 h ageing and it can be seen that this sample contains two types of particles <10 μm : calcium rich particles (yellow) and particles without calcium (pink). A higher magnification image of a couple of these particles is shown in Figure 3D. Here, the suspected tyre wear particle shows a similar morphology to the particles shown in Figure 3A, whereas the road wear particles have a slightly rougher edge. EDX spectra of these particles are shown in Figure 3E+F and here we also see that the suspected tyre wear particle has a similar elemental composition to that presented in Figure 3B, namely C, O and Si. The presence of small amounts of Al may be due to contamination from the road surface of the simulator. The suspected road wear particles again show a high concentration of Ca which is to be expected from the road simulator which uses a cement running track. The presence of these two differing particle types and the similarities in both elemental composition and morphology of one of them with TWP material suggests that nanosized T(R)WPs could be formed through environmental degradation of larger particles.

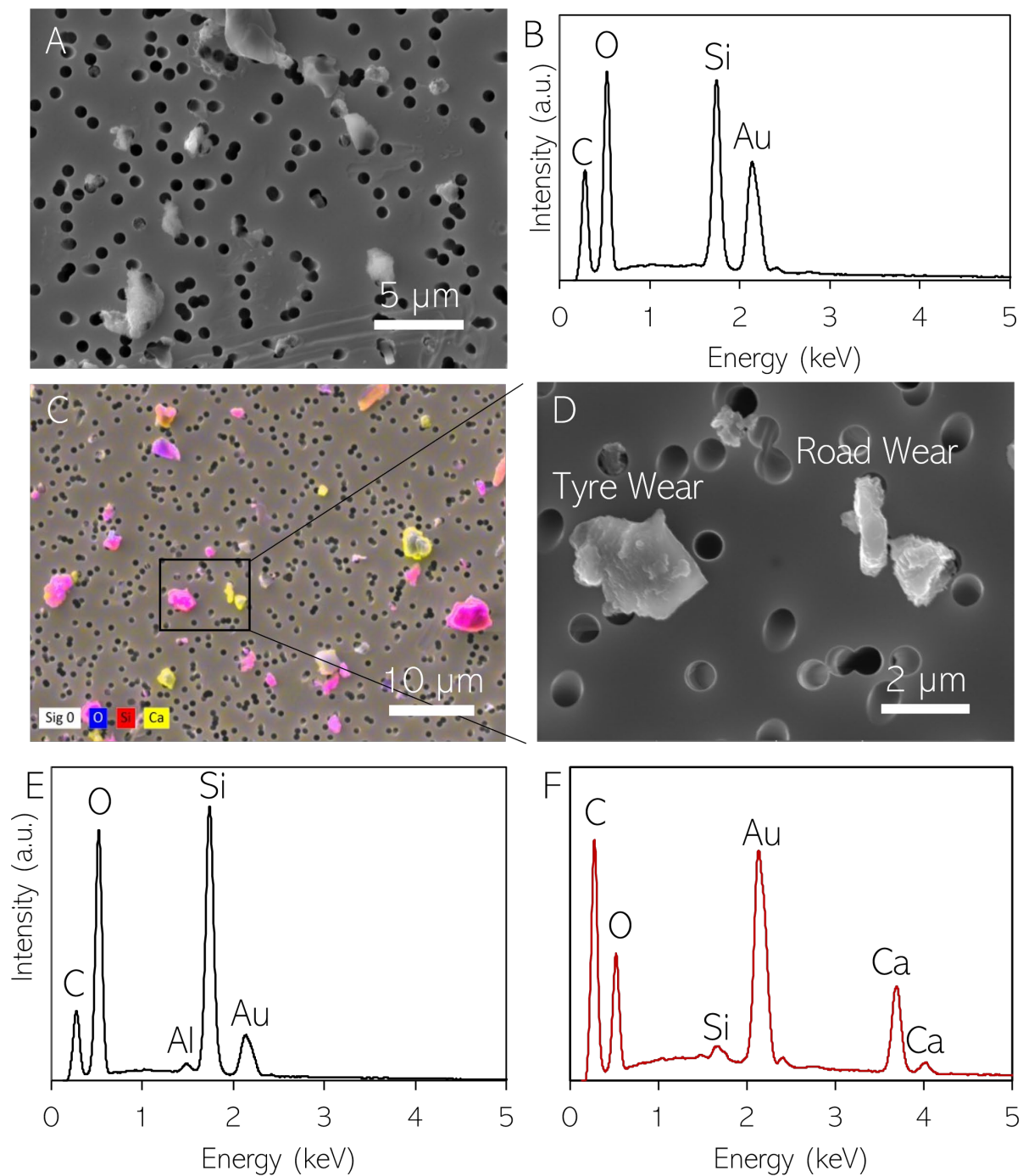


Figure 3. A. SEM image of particles <10 μm after 1000 h ageing of car TWPs; B. EDX spectrum of small car TWP particles. C. Elemental mapping of particles <10 μm in the 1000 h aged Premium TRWP sample; D. SEM image of suspected tyre wear and road wear particles indicated by the box in A; E. EDX spectrum of the suspected tyre wear particle; F. EDX spectrum of the suspected road wear particle.

Next to the analysis of particles <10 μm , SEM can also give an insight into the morphology and composition of the larger particles. When using the back scattered electron (BSE) detector, information on the composition of the particles is gained, with heavier elements appearing brighter in the image. Figure 4A+B show representative examples of a car TWP that has not been aged and a particle that has been aged for 1000 h, respectively. Looking at the morphology of the particles, it is noticeable that the aged particle is smoother than the virgin particle. This is also the case for the truck tire sample (Figure S2, Annex 5.3). When comparing the particles there is a clear difference in the

colour of the particles in the BSE images. The virgin particle is darker which means it contains more lighter atoms than the aged particle. This is also observed in the EDX spectra of the two particles, shown in Figure 4C. The virgin particle contains more carbon (C) than the aged particle, whereas the concentration of oxygen (O) and silicon (Si) are much higher in the degraded particle. The inset of Figure 4C also shows the area of the spectrum with S. S is present in low concentrations due to its use as a vulcanising agent and it remains present in cross-linking bonds of vulcanised rubber. The S seems to be present at much lower concentrations, if at all, in the 1000 h aged sample. This could suggest that UV ageing degrades cross-linkages in the rubber leading to devulcanization. This could explain the observations in Figure 1D where a shift in the decomposition temperature of synthetic rubber is observed. The C:Si ratio of fresh and 1000 h aged samples is further explored in Figure 4D.

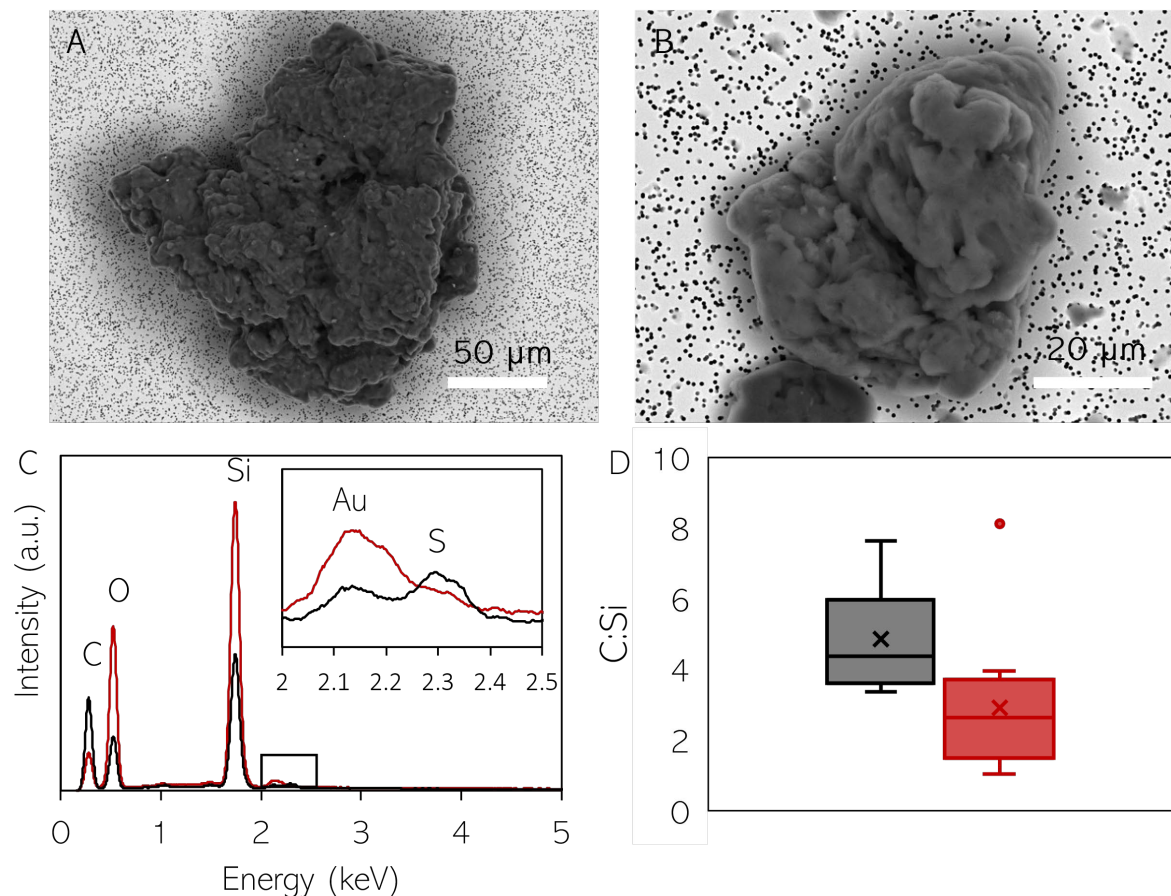


Figure 4. A. BSE image of a virgin car TWP; B. BSE image of a car TWP after 1000 h ageing; C. EDX spectra of the virgin (black) and aged (red) car TWP particles; D. Box plot of C:Si ratio of virgin (black) and aged (red) car TWP particles determined using EDX of 10 particles from each sample.

3 Conclusions

Cryomilled tyre tread and TRWPs from a road simulator were subjected to accelerated UV-ageing to simulate abiotic environmental ageing. TGA analysis of the tyre composition as a function of ageing time showed that the average degradation rate was 0.07 h^{-1} , which when corrected for accelerated ageing corresponds to an environmental degradation rate of 0.03 ($0.02 - 0.04$) day^{-1} . Natural rubber was seen to degrade quicker than synthetic rubber with the consequence that heavy duty tyres, which often contain a higher percentage natural rubber, degrade quicker than light duty tyres. Particle size was also seen to be reduced during degradation with an environmental equivalent rate of $0.03 \mu\text{m}$ ($0.02 - 0.05 \mu\text{m}$) day^{-1} . A fraction of small particles $<10 \mu\text{m}$ was also formed which was confirmed with

D3.3 UV-degradation and analysis of tyre and road wear particles (TRWP) - PU

SEM-EDX to occur for both the tyre tread and TRWP samples. This suggests that nanosized tyre wear particles may form in the environment due to degradation.

4 Bibliography

1. E. S. Rødland, S. Samanipour, C. Rauert, E. D. Okoffo, M. J. Reid, L. S. Heier, O. C. Lind, K. V. Thomas, S. Meland, A novel method for the quantification of tire and polymer-modified bitumen particles in environmental samples by pyrolysis gas chromatography mass spectroscopy. *J. Hazard. Mater.* **423**, 127092 (2022).
2. E. S. Rødland, O. C. Lind, M. J. Reid, L. S. Heier, E. D. Okoffo, C. Rauert, K. V. Thomas, S. Meland, Occurrence of tire and road wear particles in urban and peri-urban snowbanks, and their potential environmental implications. *Sci. Total Environ.* **824**, 153785 (2022).
3. C. E. Son, S. S. Choi, Preparation and Characterization of Model Tire-Road Wear Particles. *Polymers (Basel)*. **14**, 1512 (2022).
4. B. Baensch-Baltruschat, B. Kocher, F. Stock, G. Reifferscheid, Tyre and road wear particles (TRWP) - A review of generation, properties, emissions, human health risk, ecotoxicity, and fate in the environment. *Sci. Total Environ.* **733**, 137823 (2020).
5. A. E. Schwarz, S. M. C. Lensen, E. Langeveld, L. A. Parker, J. H. Urbanus, Plastics in the global environment assessed through material flow analysis, degradation and environmental transportation. *Sci. Total Environ.* **875**, 162644 (2023).
6. P. Jan Kole, A. J. Löhr, F. G. A. J. Van Belleghem, A. M. J. J. Ragas, P. J. Kole, A. J. Löhr, F. G. A. J. Van Belleghem, A. M. J. J. Ragas, P. Jan Kole, A. J. Löhr, F. G. A. J. Van Belleghem, A. M. J. J. Ragas, Wear and Tear of Tyres: A Stealthy Source of Microplastics in the Environment. *Int. J. Environ. Res. Public Health*. **14**, 1265 (2017).
7. M. L. Kreider, J. M. Panko, B. L. McAtee, L. I. Sweet, B. L. Finley, Physical and chemical characterization of tire-related particles: Comparison of particles generated using different methodologies. *Sci. Total Environ.* **408**, 652–659 (2010).
8. L. J. Knight, F. N. F. Parker-Jurd, M. Al-Sid-Cheikh, R. C. Thompson, Tyre wear particles: an abundant yet widely unreported microplastic? *Environ. Sci. Pollut. Res.* **27**, 18345–18354 (2020).
9. Y. Liu, H. Chen, J. Gao, K. Dave, J. Chen, Gap Analysis and Future Needs of Tyre Wear Particles. *SAE Tech. Pap.* (2021), doi:10.4271/2021-01-0621.
10. M. Kovoichich, J. A. Parker, S. C. Oh, J. P. Lee, S. Wagner, T. Reemtsma, K. M. Unice, S. Cheun, J. P. Lee, S. Wagner, S. C. Oh, J. P. Lee, S. Wagner, T. Reemtsma, K. M. Unice, S. Cheun, J. P. Lee, S. Wagner, Characterization of Individual Tire and Road Wear Particles in Environmental Road Dust, Tunnel Dust, and Sediment. *Environ. Sci. Technol. Lett.*, 10–17 (2021).
11. B. Baensch-Baltruschat, B. Kocher, C. Kochleus, F. Stock, G. Reifferscheid, Tyre and road wear particles - A calculation of generation, transport and release to water and soil with special regard to German roads. *Sci. Total Environ.* **752**, 141939 (2021).
12. N. Van Duijnhove, H. Denier van der Gon, J. Hulskotte, “Emissieschattingen Diffuse Bronnen Emissieregistratie-Bandenslijtage Wegverkeer-Versie Mei 2014” (Delft, The Netherlands, 2014).
13. R. Sieber, D. Kawecki, B. Nowack, Dynamic probabilistic material flow analysis of rubber release from tires into the environment. *Environ. Pollut.* **258**, 113573 (2020).
14. S. H. Cadle, R. L. Williams, Environmental Degradation of Tire-Wear Particles. *Rubber Chem. Technol.* **53**, 903–914 (1980).
15. K. M. Unice, M. P. Weeber, M. M. Abramson, R. C. D. Reid, J. A. G. van Gils, A. A. Markus, A. D. Vethaak, J. M. Panko, Characterizing export of land-based microplastics to the estuary - Part II: Sensitivity analysis of an integrated geospatial microplastic transport modeling assessment of tire and road wear particles. *Sci. Total Environ.* **646**, 1650–1659 (2019).
16. K. M. Unice, M. P. Weeber, M. M. Abramson, R. C. D. Reid, J. A. G. van Gils, A. A. Markus, A. D. Vethaak, J. M. Panko, Characterizing export of land-based microplastics to the estuary - Part I: Application of integrated geospatial microplastic transport models to assess tire and road wear particles in the Seine watershed. *Sci. Total Environ.* **646**, 1639–1649 (2019).
17. G. Wypych, *Handbook of UV Degradation and Stabilization* (ChemTec Publishing, Toronto, 2015).
18. J. Thomas, S. K. Moosavian, T. Cutright, C. Pugh, M. D. Soucek, Investigation of abiotic degradation of tire cryogrinds. *Polym. Degrad. Stab.* **195**, 109814 (2022).
19. K. M. Unice, J. L. Bare, M. L. Kreider, J. M. Panko, Experimental methodology for assessing the environmental fate of organic chemicals in polymer matrices using column leaching studies and OECD 308 water/sediment systems: Application to tire and road wear particles. *Sci. Total Environ.* **533**, 476–487

- (2015).
20. E. Corella-Puertas, P. Guieu, A. Aufoujal, C. Bulle, A. M. Boulay, Development of simplified characterization factors for the assessment of expanded polystyrene and tire wear microplastic emissions applied in a food container life cycle assessment. *J. Ind. Ecol.* **26**, 1882–1894 (2022).
 21. Y. Bar-Cohen, R. Radebaugh, Low temperature materials and mechanisms: Applications and challenges. *Low Temp. Mater. Mech.*, 437–475 (2016).
 22. D. Sun, E. Kandare, S. Maniam, A. Zhou, D. Robert, N. Buddhacosa, F. Giustozzi, Thermal-based experimental method and kinetic model for predicting the composition of crumb rubber derived from end-of-life vehicle tyres. *J. Clean. Prod.* **357**, 132002 (2022).
 23. M. Gustafsson, G. Blomqvist, I. Järlnskog, J. Lundberg, S. Janhäll, M. Elmgren, C. Johansson, M. Norman, S. Silvergren, Road dust load dynamics and influencing factors for six winter seasons in Stockholm, Sweden. *Atmos. Environ. X.* **2**, 100014 (2019).
 24. I. Järlnskog, A. M. Strömvall, K. Magnusson, M. Gustafsson, M. Polukarova, H. Galfi, M. Aronsson, Y. Andersson-Sköld, Occurrence of tire and bitumen wear microplastics on urban streets and in sweepsand and washwater. *Sci. Total Environ.* **729** (2020), doi:10.1016/j.scitotenv.2020.138950.

5 Appendix

5.1 Experimental methods and materials

Materials

Tween-20 (Sigma, Lot # SLCC6187) was used as received without further purification. All water is used was MilliQ filtered using a Millipore 0.22 µm filter. New light duty tyres were purchased from BandenConcurrent. Shredded end-of-life heavy duty tyres were provided by Rumal Tyre Recycling.

Accelerated UV-Ageing

The accelerated UV degradation was performed in an Atlas Suntester XXL, with three Xenon lamps (air cooled), a light intensity of 60 W/m² between 300 and 400 nm, relative humidity of 45% and a chamber temperature of 60 °C and a black standard temperature of 81 °C. The samples were sprayed every 12 hours for 1 minute with demi-water to remove any leachates from the rubbers, and thus mimic outdoor conditions. This sprayed water evaporated within one hour. Samples were taken after 160, 505 and 1000 h of ageing.

Milling

Small sections of tyre tread were removed from the running surface of the light duty tyres using cutting pliers. The shredded end-of-life truck tyres were used as received and may contain both running surface and sidewall rubber. These rubber chunks were then milled in a Ruhromag Retsch ZM-1 centrifugal mill with a 250 µm screen. Milling was performed under LN₂.

Fractionation

Sieving was performed in water with a drop of Tween-20 using stainless steel sieves of 53 and 200 µm. The fraction between 53-200 µm was collected and dried at 60 °C.

Static Light Scattering (SLS)

SLS was performed using a Horiba LA-960S2 in a 10 ml fraction cell equipped with a magnetic stirrer to ensure particles maintain a well-dispersed suspension. Samples were measured in a 0.05% Tween-20 in MilliQ solution to reduce agglomeration and particle-cell interactions. Particle size distributions were calculated from the scattering results using a refractive index of 2.94-0.001 (23, 24).

Scanning Electron Microscopy with Energy Dispersive X-ray Spectroscopy

SEM-EDX analyses were performed with a Tescan MAIA III Triglav field emission scanning electron microscope, equipped with Bruker XFlash Quantax 30 mm² silicon drift detectors for energy dispersive X-ray spectroscopy. SEM images were recorded in the secondary electron (SE) and backscattered electron (BSE) modes between 5 – 15 kV.

Thermogravimetric Analysis (TGA)

TGA was performed using a Mettler Toledo TGA 2 system following the method used by Son and Choi (3). The experiments were performed under nitrogen with a heating rate of 20 °C/min from 40 °C up to 750 °C before switching to air and continuing heating until 1000 °C. The mass loss with time and temperature is monitored.

5.2 Supplementary information TGA

Table S1. Triplicate measurement virgin car tires

Sample Unit	T [°C]	Run 1 [%]	Run 2 [%]	Run 3 [%]	Average [%]	St. Dev
SVOC	40-290	6.3	7.0	6.2	6.5	0.4
Pyrolysis	290-550	53.4	53.1	51.9	52.8	0.8
EC	550-1000	4.1	4.3	4.0	4.1	0.2
Inert		36.2	35.6	38.0	36.6	1.3

Table S2. Triplicate measurement virgin truck tires

Sample Unit	T [°C]	Run 1 [%]	Run 2 [%]	Run 3 [%]	Average [%]	St. Dev
SVOC	40-290	4.6	4.6	4.5	4.6	0.0
Pyrolysis	290-550	60.4	61.6	60.4	60.8	0.7
EC	550-1000	28.8	29.4	28.7	29.0	0.4
Inert		6.2	4.4	6.4	5.6	1.1

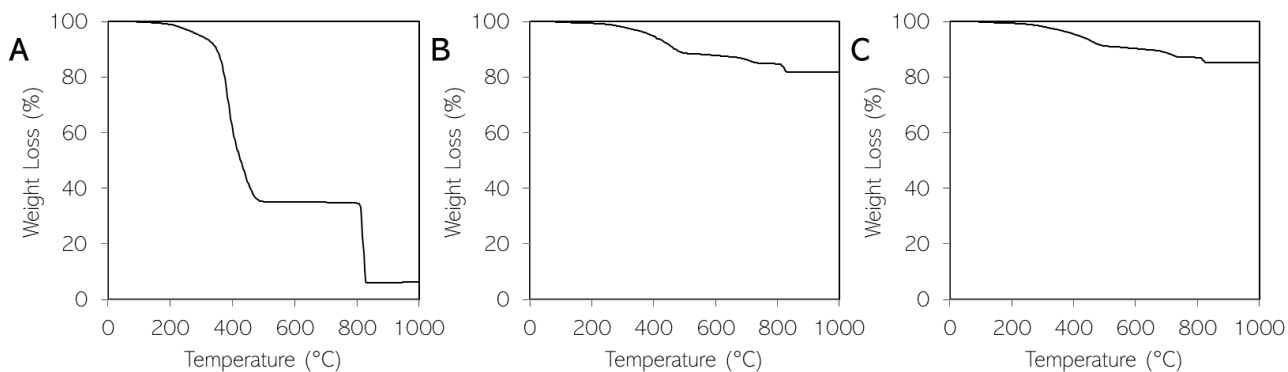


Figure S1. TGA traces of virgin **A.** Truck TWPs; **B.** Premium TRWPs; and **C.** Budget TRWPs.

5.3 Supplementary information SEM

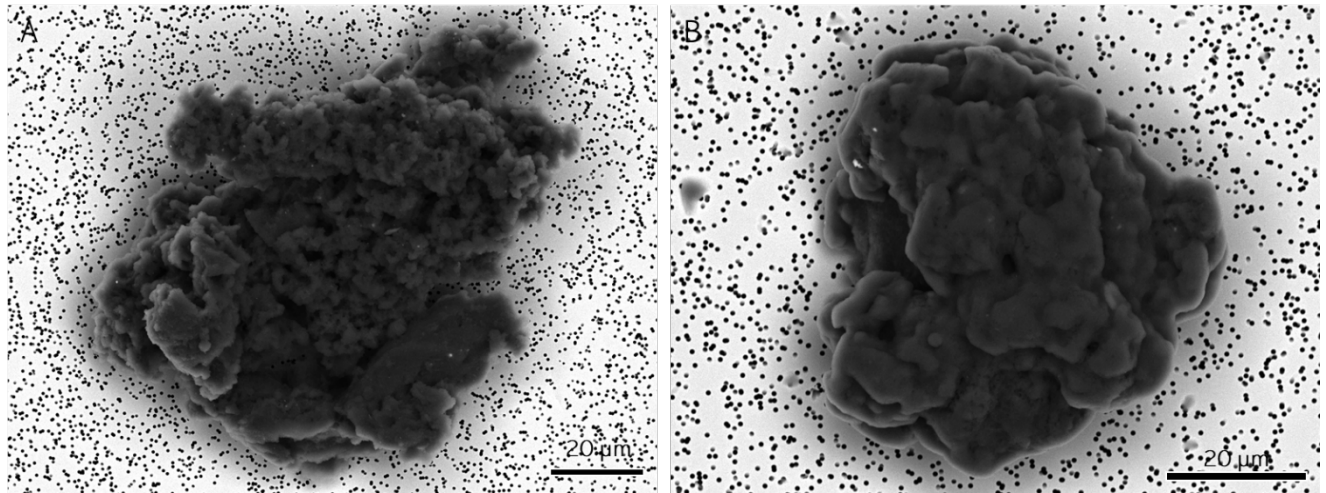


Figure S2. A. BSE image of a virgin truck TWP; B. BSE image of a truck TWP after 1000 h ageing.